

Transition to movement in granular chute flows

A. C. Santomaso*, P. Canu

Università di Padova, Istituto di Impianti Chimici, Via Marzolo 9, 35131 Padova, Italy
E-mail: andrea.santomaso@unipd.it

Abstract

This experimental investigation deals with the observation of the behaviour that dense granular materials present when they flow in steady regime on a rough chute, focusing attention on the transition to movement of the bed and on quantities involved like internal friction angle. An important aspect of the study is the identification of parameters that distinguish granular from fluid flows, aiming to verify the possibility to describe a granular bed as it was a pseudo-fluid having a particular rheological behaviour. In the experiments we have not used idealised particles (spheres, rods or disks) but sieved powders of ethylenediaminetetraacetic acid (EDTA), constituted of non-spherical particles with polydisperse size distribution and surface roughness. A static and a flowing (dynamic) layer are clearly identified. The thickness of the observed layers (static and dynamic) along the chute has been measured for different inclination, finding out that they collapse into a single curve when considered in non-dimensional scale. On the ground of the experimental data we propose a direct way of measuring the dynamic friction angle from chute observations and a simple constitutive law for granular materials in the frictional regime of motion. The law has been tested using velocity profiles obtained by filming the flowing granular bed.

1. Introduction

The study of the behaviour of granular matters has been for long time underestimated with the result that plants processing solids have low efficiency compared with those processing actual fluids (liquids and gases). Moreover there has not been any significant improvement of this situation in modern plants with respect to those built in the '60 (Morrow, 1985). The issue of fluid mechanics of granular materials is central to several processes, including silos discharge and mixing of different components. Established quantitative design criteria for such processes are sought, and they can be developed after a fundamental understanding of the mechanics of granular flow is gained.

Literature studies on fully developed stationary granular flows offer velocity and concentration profiles obtained from data on rough beds generally constituted of spherical beads. Examples of these studies are those of Savage (1979) (polystyrene beads $d_p=1.2$ mm), Ishida & Shirai (1979) (glass beads $d_p=0.4$ mm) or Drake (1988,1991) (cellulose acetate beads $d_p=6$ mm). In general experimentation lacks of data on systems made up of non-idealized powders, i.e. closer to those present in industrial applications.

Experimenters have found interesting velocity profiles but unfortunately there is no general agreement on their shape and on the behaviour of the bed. For example the velocity profiles measured by Savage (1979) and by Ishida & Shirai (1979) are

similar in the lower part, near the bottom, since they show a characteristic concave profile reversed with respect to Newtonian fluids. They differ near the free surface because of a decrease of the gradient measured by Savage and attributed to the exchange of momentum with air, while the data of Ishida & Shirai show a fairly constant gradient at the surface. Moreover these profiles are different also near the bottom from those measured by Johnson, Nott & Jackson (1990) that are approximately linear throughout the whole bed, without any significant concavity. Since the fundamental works of Bagnold (1954, 1966), attention has been paid particularly on the "grain inertia" regime (or rapid flow), with both experimental (Drake, 1988 and 1991; Savage, 1983) and theoretical works (Savage, 1979; Hayley, Norbert, & Ackermann, 1982; Campbell, 1990), but less attention has been paid on the quasi-static flow characterising the frictional regime of motion.

Gutfraind & Pouliquen (1996) studied quasi-static flow in vertical and inclined bins using a two-dimensional granular material constituted by cylindrical aluminium rods. Velocity and void ratio profiles have been measured. Pouliquen & Renaut (1996) using the same rods properly placed on a rough chute studied the onset of the flow finding a whole profile for the internal friction angle depending on the initial thickness of the bed. They performed the same experiment with glass beads and walnut shells finding similar curves and they related these profiles to the ability of granular matters to dilate during the onset of flow. Rather frequently (see for example Hsiau & Shieh (2000) or Wang & Tong (1998)) a confined flow is studied to investigate the granular flow under pure shear. Confinement limits in a way the dilatancy connected with the flow, while in many practical applications the flow of solids takes place with a free surface, as well reproduced by a chute flow.

The present work compares some of the results from the literature with new experimental data using EDTA powders, specifically addressing the onset and the regimes of granular flows. Experiments have been conducted in a parallel smooth sided chute with a no-slipping condition on the bottom. The regimes studied always include a static layer (solid-like region) below an unconfined flowing layer (fluid-like behaviour), where the coexistence of the two is considered a characteristic feature of granular materials.

The purpose of this study is the identification of suitable properties of granular materials able to characterise and distinguish their behaviour from that of 'classical' fluids. Apparently, the most suitable characteristic parameter is the internal friction angle, being this quantity directly tied with the capacity of bed to dilate. In our experiments we measured the profiles of internal static friction angle, velocity and void ratio. We also made an attempt to create a simple semiempirical model, based on the variation of the internal friction angle, trying to explain the experimental velocity profiles in the quasi-static frictional zone of the flowing bed.

2. Experimental set-up and materials

Experiments were carried out on a rough chute whose inclination could be easily changed operating on two blocking handle grips; it was constituted by a flowing channel, a feeding hopper and a collector bin (Fig. 1). The channel was made up of a wooden bottom and of two sidewalls in Perspex, 0.045 m high. It was 1.1 m long and had a variable width between 0.030 and 0.085 m. The wooden surface was

roughened by sticking on it a layer of particles identical to those used in the experiments. The layer must be renewed from time to time, because of wearing. The two parallel sidewalls were perpendicular to the bottom and made of transparent Perspex to allow the observation of the flows. One of them was fixed while the other, fixed to four L-bolts screwed on the wooden bottom, could move varying the channel width. Five observation points were displaced on the fixed free bolted wall. Four of them simply consisted of transparent graduated scales, placed respectively at 0.00, 0.23, 0.56, 0.90 m from the feeding point (that was placed at 0.10 m from the head of the chute) and were used to measure the thickness of the flowing bed. The fifth one was placed at 0.395 m from the feeding point, between the second and the third graduated scale, and consisted of a rectangular window graduated on the four sides. It was used to define the filming zone. All the significant observations about thickness have been made at 0.23 and 0.56 m from the feeding point.

The hopper had a volume of 0.02 m³ and a constant discharge hole, 0.017 m diameter wide. When it was necessary to reduce the flow we partially obstructed the discharge hole using adhesive tape. Despite the simplicity of the feeding apparatus the flow rate resulted sufficiently constant to our scope. We had not the necessity to change the feeding rate at each run and most of the experiments were carried out by reducing the discharge hole up to ½ of its area. This degree of obstruction corresponds to the mass flow rates W shown in Tab. 1 for the three particle size ranges employed. Situations in which different feeding flow rates have been used will be pointed out later in the article.

The material we used is EDTA, available in blue and white granular forms (so that the white one was used as tracer). Before the use it was sieved and only three particle size ranges were employed, i.e. $d_p=210\div 297\ \mu\text{m}$; $d_p=500\div 1000\ \mu\text{m}$ and $d_p=1400\div 2000\ \mu\text{m}$. Some flow behaviour indexes (De Jong, Hoffmann, & Finkers, 1999, Allen, 1990) like the Hausner ratio and the static angle of repose were measured, finding out that the granular material used is free flowing in each one of the three particle size ranges considered (see Fig. 2). Moreover it was measured the EDTA/Perspex friction angle and for the largest fraction it was measured also the increase of the internal friction angle close to the rough surface in the same manner as suggested by Pouliquen & Renaut (1996). The chute was set horizontally and the granular material placed on it to form a bed of constant depth; then it was slowly raised until an avalanche, corresponding to material yielding, occurred. Experiments were performed for different values of the initial thickness of the bed and the yielding angles were recorded as the internal static angle of friction for that specific thickness of the starting bed. Velocity profiles instead were determined by filming the flow with a commercial VHS camcorder (typically 30 fps) with an high speed shutter of 1/8000s. Single successive frames were digitised and analysed through a PC using the image processing software UTHSCSA Image Tool (Wilcox, Dove, McDavid & Greer 1999) and a simple movie player.

3. Observation on flow regimes and bed structure

If EDTA is fed when chute has a minimum inclination angle (about 33°) it can be observed that powder accumulates on the rough bottom causing the formation of a wedge-shaped layer of static material. This wedge grows in slope until it exceeds the

internal friction angle and then yields shifting the front of the bed forward on the chute; in other words the bed advances by mean of consecutive avalanches. This regime remembers in some aspects the slumping regime observer in slowly rotating drums (Carley-Macaulay, & Donald, 1962, 1964; Heinein, Brimacombe, & Watkinson, 1983). If the exit of the chute is reached before the wedge exceeds the side wall height, the material begins to flow in a stationary regime in which the new material fed runs over the static wedge forming a dynamic layer that reduces its thickness progressively along the chute. Accordingly, a new regime can be identified by the existence of two zone: the first one at rest (static), close to the rough bottom and the second one (dynamic) flowing on the top. The two layers are divided by an interface sufficiently clear to be distinguished with the naked eye. Interestingly when the slope of the chute is insufficient to guarantee a flowing layer, granular material provides to create itself the right flowing conditions, accumulating in a way that builds a static layer of variable height. Increasing slope, the bed runs into a chain of event that can be summed up as follows: 1) thickness of the static wedge-shaped layer reduces progressively. 2) When inclination becomes close (to an order of 2÷3 tenths of degree) to a particular angle that we call 'critical', the flowing bed enters an unstable transition state involving particularly the dynamic layer on the top. Macroscopically it has been noticed the tendency of small clusters of particles (constituted by a number of 10÷20 particles), belonging to the static layer close to interface, to set in motion simultaneously. We speak of a tendency because these clusters are extremely unstable and break up as soon as they start to move. Because of this mechanism the dynamic layer dilates and the free surface of the bed is not flat but disturbed by a series of superficial waves (tending to grow faint in proximity of the end of the chute where the bed thickness reduces and the presence of the rough rigid bottom can be felt by the top layer as well). 3) Once the critical angle is reached and exceeded, the bed displaces all its layers (static and dynamic ones) parallel to the rough bottom with the definitive vanishing of the wedge. 4) Each further increase of the inclination determines a decrease of the thickness of both layers (static and dynamic) only, with an increase of the flowing velocity, up to the disappearance of the first layer (static one) and subsequently also of the second (dynamic one) when a new regime of motion arises in the bed, characterised by a dispersed collisional flow. This regime is beyond the scope of this study, which is limited to dense granular beds only. The sequence just described qualitatively is visualised in Figures 3a and 3b for the largest EDTA size range ($d_p=1400\div 2000\ \mu\text{m}$) but similar results have been obtained for the other fractions examined. It can be clearly seen that the existence of the static wedge (3b) determines the value of the height of the interface and subsequently also of the total height of the bed (3a). For this particular size range we see that the wedge disappears at an angle of about $35.3\pm 0.1^\circ$ and the static layer (height of the interface) and the dynamic one become parallel to the rough bottom. This angle that we called critical has been found to be equal to $33.8\pm 0.1^\circ$ and $34.4\pm 0.1^\circ$, for $d_p=210\div 297\ \mu\text{m}$ and $d_p=500\div 1000\ \mu\text{m}$ respectively.

Instead of referring us to the absolute value of the static and dynamic heights it is interesting to consider their difference, that is the thickness of the superficial dynamic layer. Fig. 4 collects the dynamic layer thickness vs. chute angle for the three size ranges used. It can be seen that in correspondence of the critical angle,

previously identified, the thickness of the dynamic layer reaches its maximum. This is the consequence of the condition of instability previously discussed. Exceeding this condition the thickness of the layers decreases asymptotically to a constant value, characteristic for each particle size range.

Interestingly if we consider the thickness of the dynamic layer scaled by the mean diameter of each fraction vs. the chute inclination, we can observe that the three profiles collapse onto a single curve (Fig. 5). In particular it can be seen that this happens for inclination larger than critical one where the bed becomes independent from the cohesive forces that determined the instability and enters in a regime in which the thickness is invariant from grain dimension, assuming approximately a value of 4-5 particle diameters. We conclude that for any powder used in the experiments the thickness of the dynamic layer tends to a constant value of 5 diameters when the chute inclination exceeds the critical angles. A tendency of the three profiles to merge in a single curve also for the angles lower than the critical one seems to exist. Unfortunately data are lacking for chute slope smaller than 33° because the thickness of the bed on the chute grows above the side wall height.

In order to verify if the critical angles are an intrinsic property of the material, we performed a series of runs for each particle size range varying the feed flow rate. As can be seen in Fig. 6, showing results for $d_p=210\div297\ \mu\text{m}$, the critical angle results completely independent from mass flow rate variations, being constant in the ranges considered. Similar results have been obtained also for the other two size ranges.

Observations made on the dependence of bed behaviour on feed flow rate pointed out that the possibility to have a stationary granular flow does not depend on a minimum feed flow rate but rather on a minimum thickness of the dynamic layer. Incidentally we found out that slow stationary flows could be guaranteed only when the depth of the dynamic layer was at least 4-5 particle diameters thick but more investigations have to be done before something could be said about this.

4. Internal friction angle

The understanding of flowing bed behaviour goes through the comprehension of mechanism that define yielding and its maintenance in act. We introduced above a critical angle as the minimum one leading to the parallelism between free surface, interface and bottom. This angle seems to be independent from feed flow rate and moreover at such critical value the yielding plane is certainly determined by the interface (parallel to the chute bottom) between the two layers. According with these three observations, we identify the critical angle with the internal friction angle determined in dynamic conditions.

It's known that granular material has to dilate to flow (Reynold's dilatancy) and that in the specific case of rough chute this dilation is much more difficult close to the bottom. As pointed out by Pouliquen and Renaut (1996), the static internal friction angle changes with the initial thickness of the static bed, increasing for shallower beds. That is confirmed by our measurements as shown in Fig. 7. Such experiments were performed as described in the section 2 above, gradually raising the chute with different initial thickness of the bed. Accordingly, the static internal friction angle can be considered the sum of two contributes Gutfraind, & Pouliquen (1996):

$$\varphi_s = \varphi_{s\infty} + \beta(h) \quad (1)$$

where $\varphi_{s\infty}$ is a constant value, characteristic of the specific granular material and arises from the nature of particle surfaces in contact (frictional contribute); the second term $\beta(h)$ is function of the initial thickness of the bed, h , and it is due to the increasing difficult to dilate encountered by particles closer to the bottom of the chute (geometrical contribution). Note that yielding always starts on the surface, since it is the less constrained region. Deeper layers are progressively more constrained up the particles attached to the bottom. It is interesting to point out in this connection how far can extend the influence of the boundary in a granular material. On the other side, toward the surface, the particles are less constrained since the flowing particles above allow them to arrange a new position more freely. An empirical equation for φ_s can be obtained by fitting the measured values reported in Fig. 7. The following expression has been found:

$$\varphi_s = \varphi_{s\infty} + k_\varphi e^{-a\left(\frac{h}{d_p}\right)} = 35.146 + 14.078 e^{-0.261\left(\frac{h}{d_p}\right)} \quad (2)$$

and shown in Fig. 7 as well.

It can be immediately noticed that dynamic internal friction angle previously measured on the chute ($35.3 \pm 0.1^\circ$) is very close to the asymptotic frictional contribution $\varphi_{s\infty} = 35.146$ found in the eq. (2).

Such a coincidence is not surprising if we consider that both values refer to the same threshold between a static and a flowing condition, seen from opposite sides. More specifically, $\varphi_{s\infty}$ measures the difficulty of the particles above to set free and start flowing, while the angle of 35.3, that we call φ_{d0} with a nomenclature explained in section 6, measures the difficulty of the particles above the interface with a static layer to keep flowing. In other words both angles describe a similar condition in which the granular discrete nature of the bed material tend to vanish, assuming it to be responsible of the interlocking of the particles that prevent their movement. Indeed we identify the difficulty of grains to start moving from rest as the most notable feature of granular material.

5. Solid fraction and velocity profile

Solid fraction and velocity profiles have been reported only for the larger EDTA particles ($d_p = 1400 \div 2000 \mu\text{m}$) since the smallest particles were not so easy to observe through the movie analysis; to individuate and to follow the paths of each grain, even if for short paths, was too difficult for the fraction with $d_p = 210 \div 297 \mu\text{m}$. We limited our observations to a small range of chute inclinations aiming to isolate a precise flow regime. This is the state immediately subsequent to the phase of instability i.e. at the attainment of the internal dynamic friction angle previously described. We recall that the bed in such condition has all its layers parallel to the bottom of the chute and this represents the easiest condition to film the granular flow since the bed has the minimum inclination to which the parallelism is guaranteed and consequently the lower speed and larger thickness.

The possibility to observe the flow through the transparent sidewalls allows us to have an idea of the distribution of the particles in movement. Although in a bidimensional perspective, an evaluation of the volumetric fraction of solid as a function of the depth in the bed can be obtained. Note that in such a way it is possible to determine the solid fraction under flow conditions. An example is shown in Fig. 8. A certain experimental uncertainty is evident, but it is also evident the existence of a profile, suggested by the dashed line. As it can be seen, the mean volumetric fraction of solid ν in the static layer remains close to 0.74 that is the maximum value for packed spheres. Then, approximately at about 2 granular diameter from the bottom, the bed starts moving and the dilation causes a dispersion of ν until a depth of 5÷5.5 diameters. This behaviour can be attributed to the presence of the frictional zone where grains are in a quasi-static regime of motion characterised by an exchange of momentum mainly by mean of their mutual rubbing. The motion observed in this layer results to be similar to that described by Gutfraind & Pouliquen (1996) characterised by notable fluctuations of velocity both in intensity and direction with accelerations, sudden decelerations and even temporary at rest. This behaviour explains the dispersion of data by the presence of zone of instantaneous accumulation close to others suddenly empty. Fig. 8 shows an upper zone where data describe a well-defined profile. Note that the solid fraction starts at a value of 0.6 and decreases quickly to a value close to 0.3. It is well known indeed that higher velocities of the granular bed are connected with larger void fractions. Similarly to the fraction of solid, the velocity measurements at the sidewall do not represent what happens inside the bed, but they can provide useful qualitative information on the behaviour of the granular material. We have at our disposal the velocity profiles of the two larger fractions of particles and we will pay particular attention on the fraction 1400÷2000 μm again, since it has the double advantage of flowing more slowly and being less affected by the wall friction (see Tab. 2) making easier the analysis of the pictures and more meaningful the data. In Fig. 9 we can see two velocity profiles referring to the two size ranges considered ($d_p=500\div1000$ μm and $d_p=1400\div2000$ μm), for different chute inclination (33.5° and 35.3° respectively), while the width of the channel remains constant (0.03 m). It can be immediately noticed in both cases a static layer of finite depth at rest close to the bottom. A constant thickness of this non-flowing layer along the chute depends on the attainment along the yielding plane of the internal friction angle previously described. The second thing that appears evident from both profiles is that they are convex in the direction of flow. In other words the velocity gradient apparently increases constantly approaching the surface. It is well known that other fluids like Newtonian or viscoplastic, in laminar regime show a concave velocity profile that becomes a perfect parable for Newtonian. Note that viscoplastic bear some similarity with our case in that they describe the behaviour of mud, a material constituted by two distinguished phases, one fluid and the other solid although very minute. Not many published experimental works report observed velocity profiles and, as previously said, no general agreement is reached on their shape. Unfortunately our data in the upper part of the bed are rather uncertain, particularly for the highest velocities measured with the larger inclination of the chute. This is a consequence of the measurement technique limited by a frame rate of only 30 frames per second. Because of this, we can not firmly confirm one of the two behaviours previously seen

in literature (Savage, 1979, Ishida & Shirai, 1979) in the upper part of the flowing bed. We will therefore pay particular attention on the underlying layers that are perhaps more important in order to understand the mechanism of flowability. They contain the transition between the static and the quasi-static regime of motion and the transition between the quasi-static and the rapid flow regime.

In these lower regions of the bed our data (Fig. 9) seem to confirm those profile of literature having a reverse concavity (with respect to the Newtonian fluids) (Savage, 1979, Ishida & Shirai, 1979). However other profiles picked up at lower inclinations and with smaller flow velocity have accentuated a behaviour that not appeared so evident in Fig. 9. From Fig. 10 it can be observed that the profile is not so smooth as appeared in a first sight for the presence of an abrupt increase of velocity gradient in correspondence of a depth of about 5 particle diameters, with the following part of the profile assuming a linear shape. Such transition belongs to a range of ordinate coinciding with the end of the dispersion zone of the fraction of solid v (Fig. 8). We let this dispersed zone, corresponding to the convex part of the velocity profile, to coincide with a frictional zone of about 4-5 particle diameters in thickness.

6. A semiempirical mathematical model of the friction layer

In the following we attempt to develop a simple model able to reproduce the observed reverse concavity of the velocity profiles. The model is based on a few hypotheses suggested by the experimental measurements. We treat our granular system as a continuum to describe it through the classical equations of motion for a continuum. For this purpose it is necessary to state a constitutive law able to predict the rheologic behaviour of the particle bed as a whole. For a Newtonian fluid this law gives the definition of viscosity. For granular systems we try to formulate a constitutive law based on a variable pseudo-viscosity. We focused our attention on the role played by dilatancy in determining the motion in the lower layers of the bed, in the frictional zone. We used the internal friction angle as the property characterising the pseudo-viscous term. The hypothesis at the base of the model is that the measured critical angle, φ_d , is one of the infinite values that a dynamic layer shows through its depth. Specifically, φ_d is the maximum of these values at the bottom of the dynamic layer, i.e. the interface between static and dynamic layers. In other words we suppose that φ_d varies inside the dynamic layer following a law similar to φ_s in static conditions. While φ_s varied as a function of the initial depth of the bed (different for each run), here φ_d varies inside the same bed, but for reasons and mechanisms that are similar to those discussed above, to explain the behaviour of static beds. Particularly, we suppose that φ_d increases towards the interface between static and dynamic layer, because of the increased difficult of the bed to maintain dilation, with the same law as φ_s increases towards the rigid bottom, because of the increased difficult of the bed to start dilation. In the case of the dynamic internal friction angle a law similarly to equation (2) can be formulated as:

$$\varphi_d = \varphi_{d\infty} + k_{\varphi_d} e^{-\beta \left(\frac{x}{d_p} \right)} \quad (3)$$

where β and k_{φ_d} are constants.

However, if the inability of grains to start flowing depends on the absolute value of the static internal friction angle (Pouliquen & Renaut, 1996), the ability to maintain a relative motion between two adjacent dynamic layers, we believe that must depend on the variation of the dynamic internal friction angle, and specifically on its decrease, instead of its value. A decrease is required to explain bed yielding along several granular layers instead of a single plane, as observed in the frictional zone. To explain this concept, suppose to have three adjacent granular layers as in Fig. 12, with the lower one static and rigid. For simplicity, we assume that grains do not rotate nor break the line they belong to, which is true considering a sufficiently short path. If the layer immediately above the lower one moves (dilating) it means that the internal static friction angle has been exceeded at the contact plane between the two layers. The third layer, instead, to move simultaneously and maintain itself in motion with respect to the second one, it must experience, at the interface with the second layer, a friction angle necessary lower than the previous layer. Furthermore the tendency of grains to set free and move is directly proportional to the decrease of the friction angle between two adjacent layers, so that the flowability in the shear zone depends mainly on the gradient $d\varphi_d/dx$ and not on the absolute value of φ_d .

If $d\varphi_d/dx$ is directly proportional to the ability of flowing of the material and since we want to create a pseudo-viscous term opposing the flowability, we suggest an expression for the pseudo-viscosity of the form:

$$\mu'(\varphi) = \frac{k_\mu}{\left| \frac{d\varphi}{dx} \right|} \quad (4)$$

where k_μ is a constant.

In the rapid flow zone, as pointed out for example by Bagnold (1954), or Savage (1983), the dependence of τ from du_z/dx is of the second order because the momentum transfer during the collision characterising this regime of motion and the collisional frequency are both proportional to the relative velocity of the colliding grains. In the frictional zone below, the momentum is transferred mainly by the superficial rubbing of the grains in close contact and results proportional simply to the number of contacts per time unit so that we can assume a first order dependency on the velocity gradient

$$\tau_{xz} = -\mu'(\varphi_d) \frac{du_z}{dx} \quad (5)$$

for the pseudo-viscous component of the shear stress. Note that this term is a function of dilation and velocity.

In addition to the dynamic considerations above, we have to consider the capacity of the granular bed to sustain internal stresses in static conditions. For this reason the expression for τ have to contain a term similar to that of Bingham's fluids to account for an initial stiffness of the material. In the case of granular material, such a minimum stress must depend on the depth in the bed, being proportional to the normal stress. This terms is generally related to the yielding stress according to the Coulomb criterion that for cohesionless materials gives:

$$\frac{\partial \tau_{xz}}{\partial x} = -\rho g \sin \theta \quad (6)$$

Yielding will occur along the plane where τ reaches a value equal to the product of the normal stress σ with the tangent of φ_* , where φ_* represents a static internal friction angle. As previously seen the value of this angle is not unique. To choose a value we consider that the bed will start to yield along the plane distant x_1 from the bottom where static internal friction angle is minimum. This is the same to say that motion in the bed will stop at a depth from the surface equal to x_2 when the dynamic internal friction angle becomes maximum. Since x_1 and x_2 individuate the same plane and the two angles, as we have seen previously, coincide with a common value of 35.146° ($d_p=1400\div 2000 \mu\text{m}$), we will use $\varphi_*=\varphi_{d0}\equiv\varphi_{s\infty}$ in equation (6), with $\varphi_{s\infty}$ being the asymptotic (minimum) value of φ_s in eq. (1) and φ_{d0} the maximum value of φ_d , at the interface between static and flowing layers.

Putting together the two contributions above we can write the general expression expected for the shear stress:

$$\tau_{xz} = \tau_{xz}(\varphi_{s\infty})_{Coulomb} - \mu'(\varphi_d) \frac{du_z}{dx} \quad (6)$$

Frictional term Pseudo-viscous term,
 depending on dilation but depending on dilation and
 not depending on velocity on velocity

At this point we have all the elements necessary to construct the equation of motion that integrated will give the velocities profiles sought. Assuming the flow to be steady and uniform along the z axis (Fig. 13) we can write the equations of motion that for our chute become:

$$\frac{\partial \tau_{xz}}{\partial x} = -\rho g \sin \theta. \quad (7)$$

$$\frac{\partial \sigma_{xx}}{\partial x} = -\rho g \cos \theta \quad (8)$$

Integrating with the condition at $x=0$ (the beginning of the dynamic layer, cf. Fig. 13):

$$\tau_{xz}(0) = \tau_{yield}$$

$$\sigma_{xx}(0) = \sigma_{yield}$$

where τ_{yield} and σ_{yield} are the stresses at the onset of flow, we obtain:

$$\tau_{xz}(x) = \tau_{yield} - \rho g x \sin \theta \quad (9)$$

$$\sigma_{xx}(x) = \sigma_{yield} - \rho g x \cos \theta \quad (10)$$

For the Mohr-Coulomb yielding criterion of eq. (5) we have that:

$$\tau(\varphi_{s\infty})_{Coulomb} = \tan \varphi_{s\infty} \sigma_{xx} = k_\tau (\sigma_{yield} - \rho g x \cos \theta) \quad (12)$$

where $\tan \varphi_{s\infty} = k_\tau$. Now eq. (9) and eq. (6) can be compared, resulting in:

$$\tau_{yield} - \rho g x \sin \theta = k_\tau (\sigma_{yield} - \rho g x \cos \theta) - \frac{k_\mu}{\left| \frac{d\varphi_d}{dx} \right|} \frac{du_z}{dx} \quad (13)$$

Since $\tau_{yield.} = k_{\tau} \sigma_{yield.}$ and $\left| \frac{d\varphi_d}{dx} \right| = k_{\varphi_d} \frac{\beta}{d_p} e^{-\beta \left(\frac{x}{d_p} \right)}$, eq. (13) reduces to:

$$\rho g (\sin \theta - k_{\tau} \cos \theta) x = \frac{k_{\mu}}{k_{\varphi_d}} \frac{d_p}{\beta} e^{\beta \left(\frac{x}{d_p} \right)} \frac{du_z}{dx} \quad (14)$$

that is:

$$\frac{du_z}{dx} = \frac{k_{\varphi_d}}{k_{\mu}} \rho g (\sin \theta - k_{\tau} \cos \theta) x \frac{\beta}{d_p} e^{-\beta \left(\frac{x}{d_p} \right)}, \quad (15)$$

It can be observed that the velocity gradient according to eq. (15) is zero at $x=0$ and is expected to increase with x because all the coefficients are positive, as shown by the experimental profiles. The factor $(\sin \theta - k_{\tau} \cos \theta)$ must be positive since the condition

$$\sin \theta - k_{\tau} \cos \theta = 0$$

uniquely identifies the critical angle below which the bed doesn't flow:

$$k_{\tau} = \frac{\sin \theta}{\cos \theta} \Big|_{\text{critical}} = \tan \varphi_{s\infty}$$

that turns out to be exactly the static internal friction angle, $\theta_{critical} = \varphi_{s\infty}$.

Integrating (15) with the boundary condition $u_z=0$ at $x=0$ we finally obtain:

$$u_z = \frac{k_{\varphi_d}}{k_{\mu}} \frac{d_p}{\beta} \rho g (\sin \theta - k_{\tau} \cos \theta) \left\{ 1 - e^{-\beta \left(\frac{x}{d_p} \right)} \left[\beta \left(\frac{x}{d_p} \right) + 1 \right] \right\}, \quad (16)$$

which represents the velocity profile for the friction zone. This equation, for the hypotheses done, doesn't describe properly the motion in the upper layers of the bed, where the mechanism is essentially collisional instead of frictional.

In Fig. 11 it can be seen that equation (16) fits the experimental data quite well in the frictional zone showing the characteristic concave profile while in the upper part diverges significantly from the experimental data. Data fitting provides the values for the unknown parameter β and for the ratio k_{φ_d}/k_{μ} that characterise the profile of the dynamic internal friction angle and are respectively 0.07 and 0.01. With the estimated parameters we can check the profile of the dynamic internal friction angle. Fig. 14 shows a comparison between the variation of the two internal friction angles. It can be seen that the $\varphi_d(x)$ profile is almost linear through the bed because the fitted value of β is small. A small gradient for the dynamic friction angle with the depth of the bed was expected indeed since the effort to maintain dilation to keep flowing is smaller than the effort to create it (in order to start flowing).

7. Conclusions

In this work we investigated the behaviour of flowing granular bed. We started from experimental observations in a range of inclination corresponding to the situation in which the bed flow overcomes a condition of instability and becomes steady,

displacing its static and dynamic layers parallel to the chute bottom. We have systematically measured the thickness of the dynamic layer vs. chute inclination for three different flowing beds made of particles belonging to different size range and observing that in non-dimensional scale the obtained profiles collapse into a single curve. The curve presents a marked maximum in correspondence of the angles in which the bed goes through the mentioned instability. We have seen how these angles are not depending upon imposed external condition such as feeding rate but are characteristic of the particle size. Starting from measured profiles of the internal friction angle along bed depth in static condition we suggested the existence of a similar profile for the friction angle in the dynamic situation as well. In this case, measured critical angle was nothing else but the dynamic internal friction angle measured at the bottom of the dynamic layer and was very close to the value of friction angle measured in static condition at the top of the static granular bed. Moreover, velocities profiles have been measured. In order to explain their reversed concavity (with respect to Newtonian fluids) we have constructed a simple mathematical model using a constitutive law for granular materials based on the variation of the dynamic internal friction angle. The model closely fit the experimental velocity profiles in the frictional zone.

List of symbols

d_p	Particle diameter.
k_ϕ	Parameter in internal static friction angle expression.
k_μ	Parameter in internal static friction angle expression.
$k_{\phi d}$	Parameter in internal dynamic friction angle expression.
k_τ	Tangent of the internal friction angle.
g	Gravity
h	Bed thickness
u_z	Velocity along the chute
α	Empirical coefficient in internal static friction angle expression.
β	Parameter in internal dynamic friction angle expression.
$\beta(h)$	Geometrical contribution to internal static friction angle.
δ	Frictional zone thickness.
θ	Chute inclination
μ	Viscosity.
$\mu'(x)$	Pseudo viscosity.
v	Void ratio.
ρ	Density.
σ_{xx}	Normal stress.
τ_{xz}	Tangential stress.
ϕ_s	Internal static friction angle.
$\phi_{s\infty}$	Frictional contribution to internal static friction angle.
ϕ_d	Internal dynamic friction angle.
ϕ_{d0}	Internal dynamic friction angle at the yielding plane.

References

- Allen T., *Particle size measurement*, Chapman and Hall, London (1990).
- Bagnold, R. A. (1954) Experiments on a gravity-free dispersion of large solid spheres in a Newtonian fluid under shear. *Proc. Roy. Soc. A*, **225**, pp. 49÷63.
- Bagnold, R. A. (1966) The shearing and dilatation of dry sand and the 'singing' mechanism. *Proc. Roy. Soc. A*, **295**, pp. 219÷232.
- Campbell, C.S. (1990) Rapid granular flow. *Annu. Rev. Fluid Mech.* **22**, pp. 57÷92.
- Carley-Macaulay, K.W. & Donald, M.B. (1962) The mixing of solids in tumbling mixers: I. *Chem. Eng. Sci.* **17**, 493.
- Carley-Macaulay, K.W. & Donald, M.B. (1964) The mixing of solids in tumbling mixers: II. *Chem. Eng. Sci.* **19**, 191.
- De Jong, J. A. H., Hoffmann, A. C. & Finkers, H. J. (1999) Properly determine powder flowability to maximize plant output. *Chem. Eng. Progress*, April 1999, pp.25÷34.
- Drake, T.G. (1988) Experimental flows of granular material. *Ph. D. Thesis*, University of California, Los Angeles.
- Drake, T.G. (1991) Granular flow: physical experiments and their implications for microstructural theories. *J. Fluid Mech.* **225**, pp.121÷152.
- Gutfraind, R. & Pouliquen, O. (1996) Stress fluctuations and shear zones in quasi static granular chute flows. *Phys. Rev. E* **53**, pp.552÷561.
- Hayley, S., Norbert, L. & Ackermann, M (1982) Constitutive relationships for fluid-solid mixtures. *J. Eng. Mech. Div.*, ASCE, **108**, No.EM5, pp. 748÷763.
- Heinein, H., Brimacombe, J.K. & Watkinson A. P. (1983) Experimental study of transverse bed motion in rotary kilns. *Met. Trans. B*, **14B**, 191.
- Hsiau, S. S. & Shieh, Y. M. (2000) Effect of solid fraction on fluctuations and self-diffusion of sheared granular flow. *Chem. Eng. Science* **55**, pp.1969÷1979.
- Ishida, M. & Shirai, T. (1979) Velocity distributions in the flow of solid particles in an inclined open channel. *J. Chem. Eng. Japan* **12**, pp.45÷50.

Santomaso, A.C., Canu, P. Transition to movement in granular chute flows (2001)
Chemical Engineering Science, 56 (11), pp. 3563-3573.
DOI: [10.1016/S0009-2509\(01\)00026-4](https://doi.org/10.1016/S0009-2509(01)00026-4)

- Johnson, P.C., Nott, P. & Jackson, R (1990) Frictional-collisional equations of motion for particulate flows and their application to chutes. *J. Fluid Mech.* **210**, pp.501÷535.
- Merrow, E.W. (1985) Linking R&D to problems experienced in solids processing. *Chem. Eng. Progress* **81**, pp.14÷22.
- Pouliquen, O. & Renault, N. (1996) Onset of granular flows on an inclined rough bed: dilatancy effects. *Journal de Physique II* **6**, pp.923÷935.
- Savage, S.B. (1979) Gravity flow of cohesionless granular materials in chutes and channels. *J. Fluid Mech.* **92**, pp.53÷96.
- Savage, S.B. (1983) granular flow at high shear rates. In *Theory of dispersed multiphase flow* (ed. Richard E. Meyer), Academic Press, pp.339÷358.
- Wang, C.,H. & Tong, Z. (1998) Transient development of instabilities in bounded shear flow of granular materials. *Chem. Eng. Science* **53**, pp.3803÷3819.
- Wilcox, C. D., Dove, S. B., McDavid, W. D. & Greer, D. B. (1999) UTHSCSA Image Tool Version 2.00, University of Texas, San Antonio, Texas.

Table 1 Dependence of mass flow rate from particle size ranges.

Particle size ranges (μm)	Mass flow rate W (kg/s)
210÷297	0.0438
500÷1000	0.0373
1400÷2000	0.0301

Table 2 Measured critical angle θ_c and EDTA/Perspex friction angle.

Particle size ranges (μm)	Critical angle θ_c	EDTA/Perspex friction angle
210÷297	33.8±0.1°	34.9±0.1°
500÷1000	34.3±0.1°	29.5±0.1°
1400÷2000	35.3±0.1°	24.8±0.1°

Figure Captions

Figure 1: Experimental set-up.

Figure 2: Flowability of EDTA powders used.

Figure 3: Variation of the total depth of the bed 3a) and of the interface height (i.e. the static thickness) 3b) with the chute inclination. Data refers to $d_p=1400\div 2000 \mu\text{m}$.

Figure 4: Dynamic layer thickness vs. chute inclination. \square - $d_p=210\div 297 \mu\text{m}$; \blacktriangle - $d_p=500\div 1000 \mu\text{m}$; \blacksquare - $d_p=1400\div 2000 \mu\text{m}$.

Figure 5: Non-dimensional dynamic layer thickness vs. chute inclination. \square - $d_p=210\div 297 \mu\text{m}$; \blacktriangle - $d_p=500\div 1000 \mu\text{m}$; \blacksquare - $d_p=1400\div 2000 \mu\text{m}$.

Figure 6: Invariance of critical angle with feed flow rate: \square - $W=13.6 \text{ g/cm}^3$; \blacklozenge - $W=22.7 \text{ g/cm}^3$; \blacktriangle - $W=47.3 \text{ g/cm}^3$.

Figure 7: Variation of the internal static friction angle vs. the non-dimensional bed depth h/d_p with $d_p=1400\div 2000 \mu\text{m}$. Experimental data and mathematical expression.

Figure 8: Variation of volumetric fraction of solid with bed depth. Data refers to $d_p=1400\div 2000 \mu\text{m}$; $\theta=35.3^\circ$; chute width $w=30 \text{ mm}$.

Figure 9: Velocity profiles: a) $d_p=500\div 1000 \mu\text{m}$; $\theta=34.5^\circ$; b) $d_p=1400\div 2000 \mu\text{m}$; $\theta=35.3^\circ$. Width $w=30 \text{ mm}$ constant.

Figure 10: Velocity profile considered without the static layer. Profile refer to: EDTA $d_p=1400\div 2000 \mu\text{m}$; chute inclination $\theta=35.3^\circ$; channel width $w=30 \text{ mm}$; feed flow rate $W=0.0301 \text{ kg/s}$.

Figure 11: Lower portion of the velocity profiles in non-dimensional scale. Profile refer to: EDTA $d_p=1400\div 2000 \mu\text{m}$; chute inclination $\theta=35.3^\circ$; channel width $w=30 \text{ mm}$; feed flow rate $W=0.0301 \text{ kg/s}$.

Figure 12: Mechanism for dilation and consequent shearing between three adjacent particle layers.

Figure 13: Schematic view of the coordinate system chosen and of the velocity profile in the bed.

Figure 14: Comparison between the static internal friction angle experimentally found and the dynamic one partially extrapolated from the model.

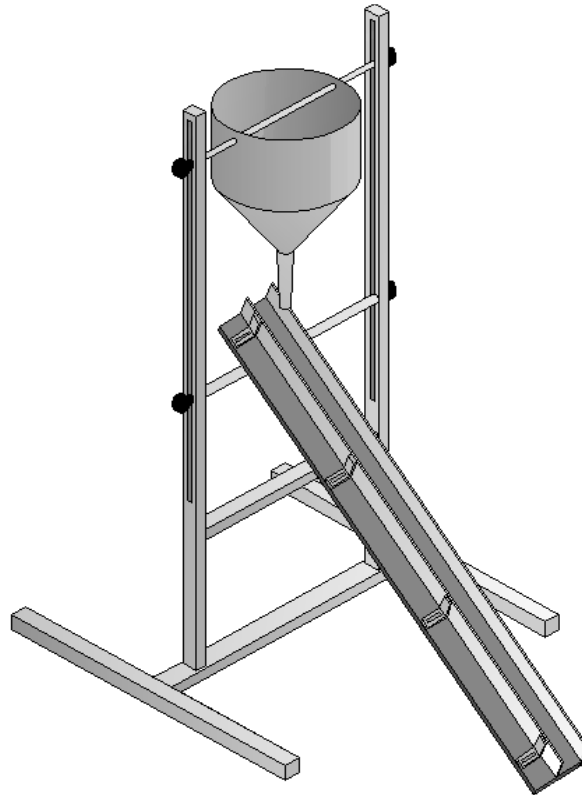


Figure 1

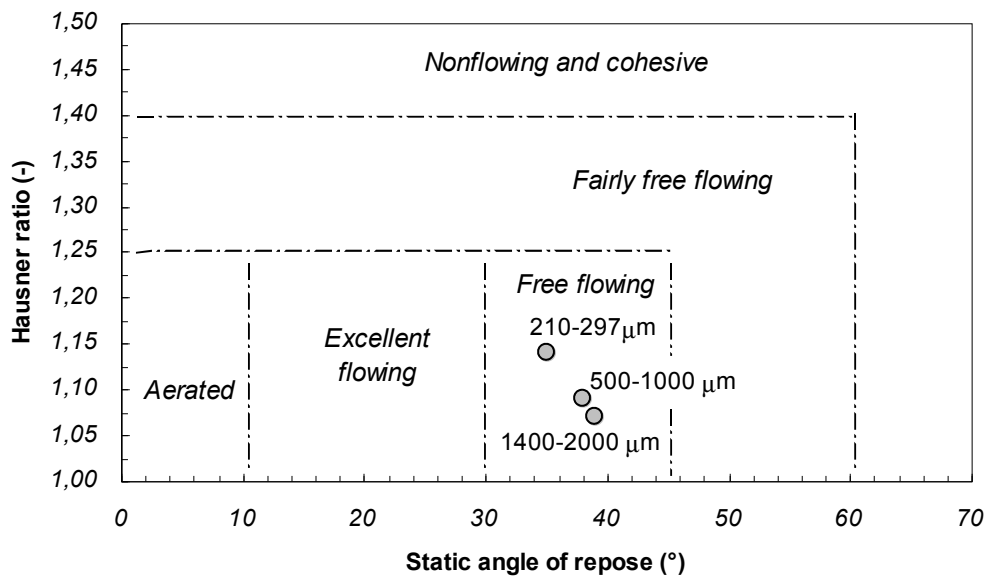


Figure 2

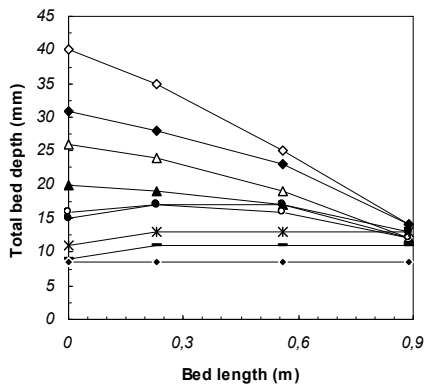


Figure 3a

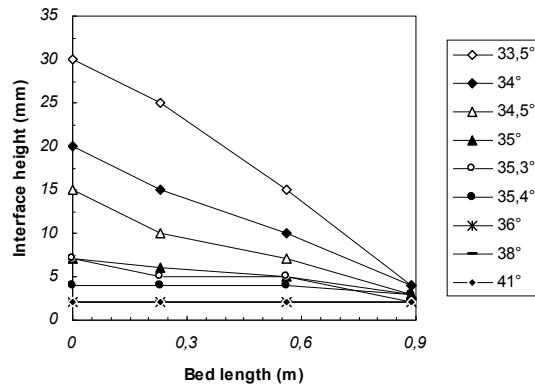


Figure 3b

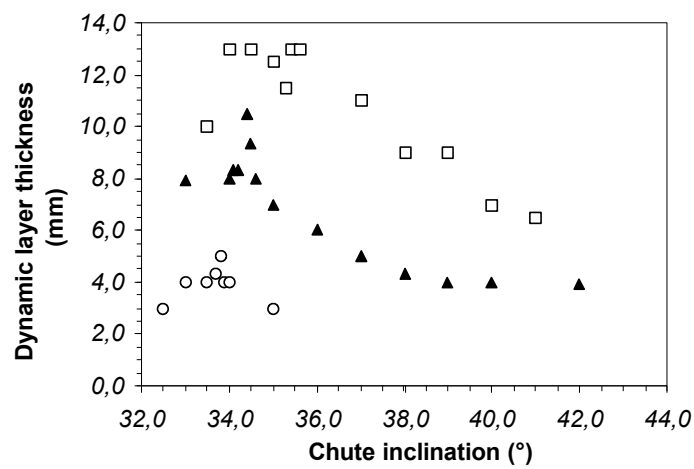


Figure 4

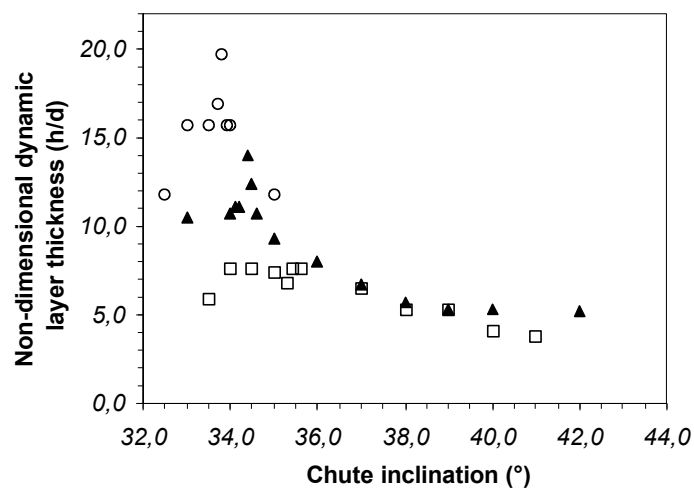


Figure 5

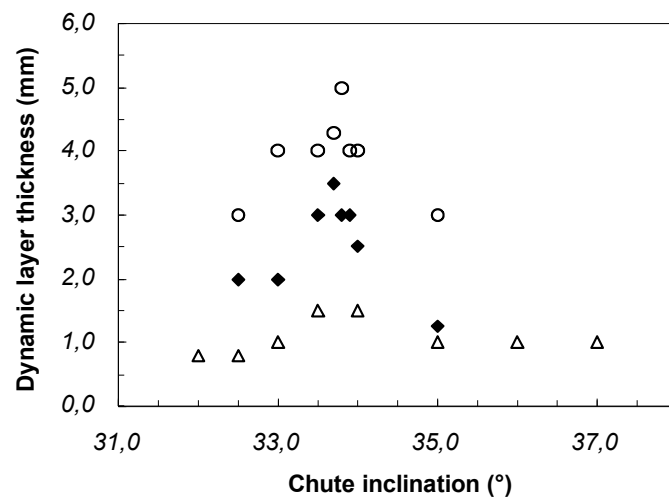


Figure 6

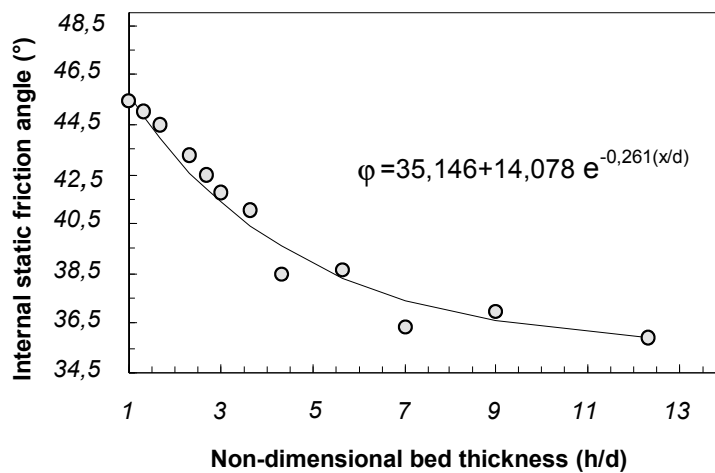


Figure 7

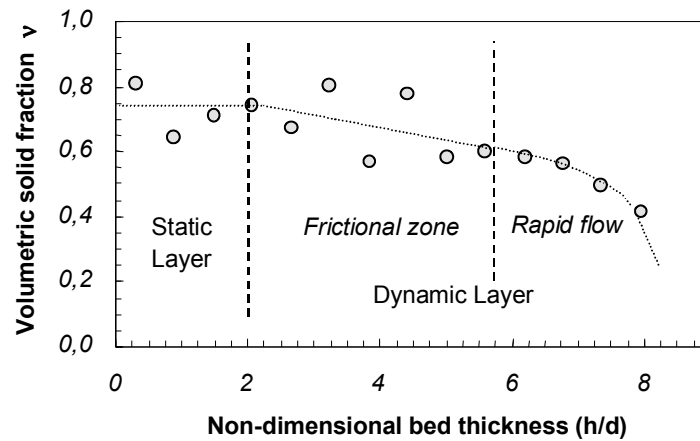


Figure 8

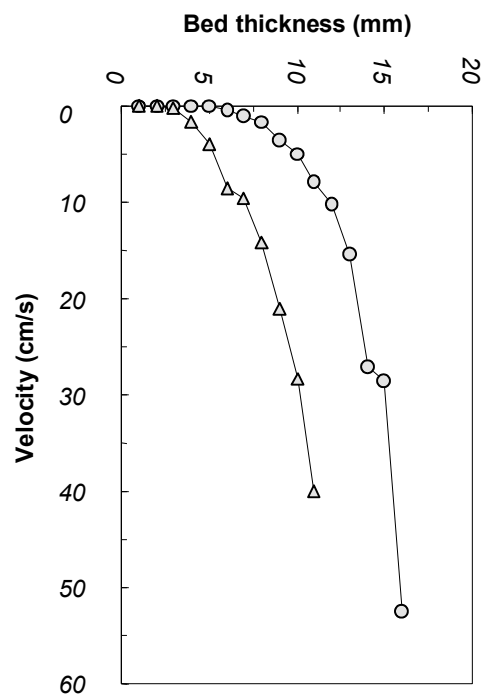


Figure 9

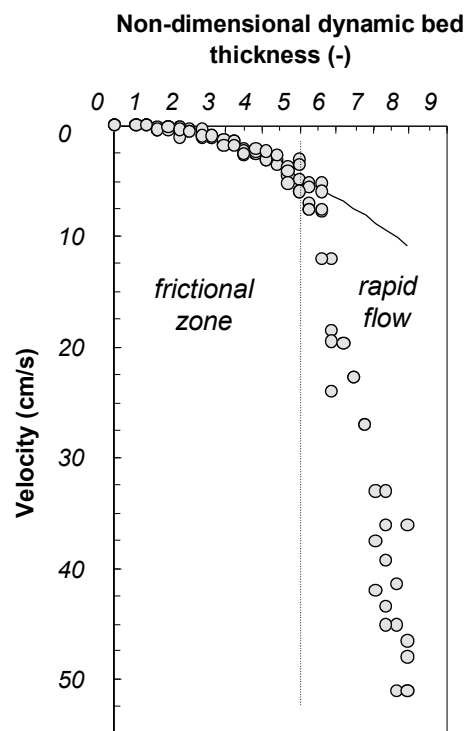


Figure 10

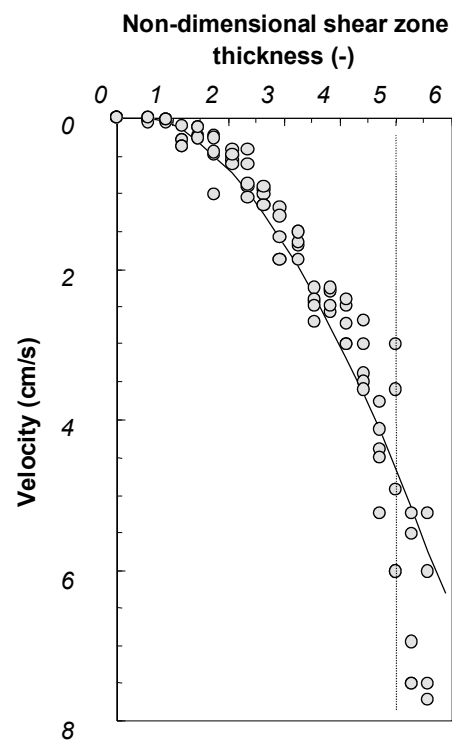


Figure 11

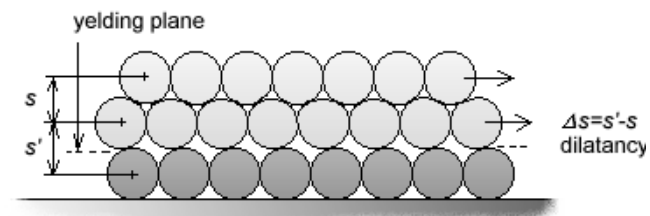


Figure 12

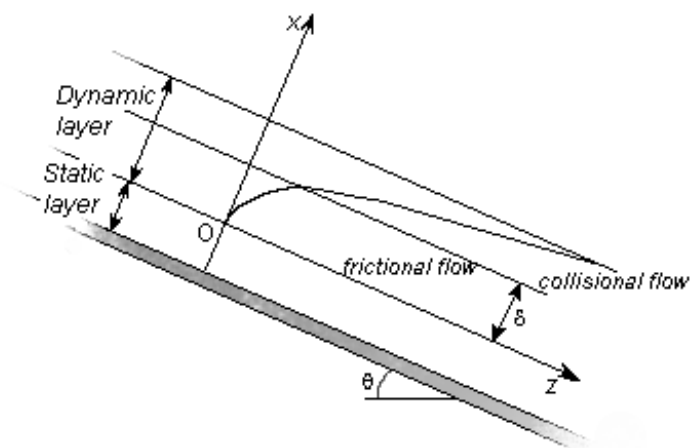


Figure 13

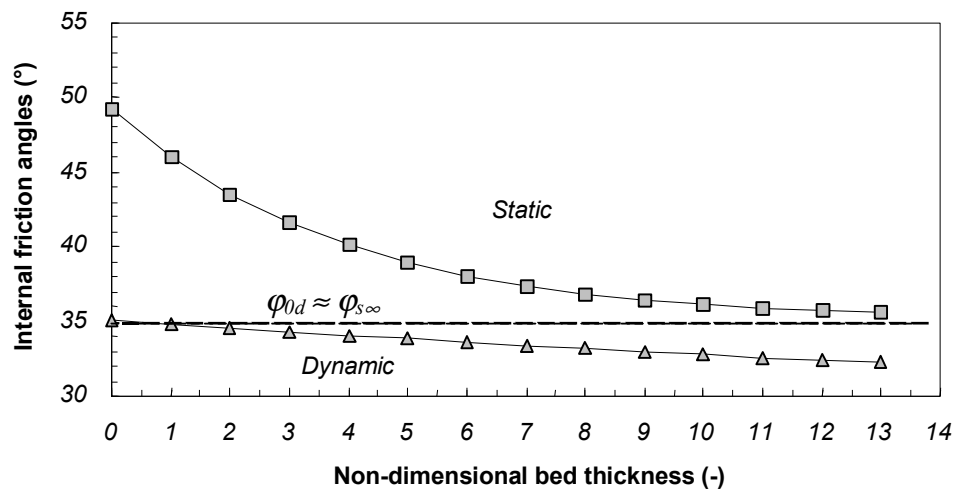


Figure 14